Physica B 431 (2013) 6–10

Contents lists available at ScienceDirect

Physica B

journal homepage: www.elsevier.com/locate/physb

Phase transition induced double-Gaussian barrier height distribution in Schottky diode

A. Bobby [a,*], S. Verma [b], K. Asokan [b], P.M. Sarun [a], B.K. Antony [a]

[a] Department of Applied Physics, Indian School of Mines, Dhanbad 826004, India
[b] Inter University Accelerator Center, Aruna Asaf Ali Marg, New Delhi 110067, India

ARTICLE INFO

Article history:
Received 12 July 2013
Received in revised form
21 August 2013
Accepted 24 August 2013
Available online 31 August 2013

Keywords:
Hg–*n*Si Schottky contacts
Interfacial conduction mechanism
Inhomogeneity

ABSTRACT

The charge transport mechanisms of Hg contact on *n*-type silicon crystal having ⟨1 0 0⟩ orientation were investigated in the temperature range of 160–293 K by the thermionic emission theory. The temperature variation of barrier height and ideality factor illustrates an inhomogeneous interface with a Gaussian barrier height distribution. The plots of temperature dependent zero-bias barrier height, ideality factor, series resistance and reverse leakage current show a discontinuity below 240 K. The experimental barrier height and ideality factor versus $1/T$ plot gives two slopes, one in the 160–220 K region and the other in the 240–293 K region, thereby revealing a double Gaussian distribution of barrier heights. The observed discontinuity in the diode parameters and the existence of double Gaussian barrier heights are interpreted on the basis of phase transition of mercury from its liquid state to solid form.

1. Introduction

Rectifying metal–semiconductor junctions, popularly known as Schottky contacts, have been a subject of intense study for many years due to its significance in electronic industry. The most important electrical property of this structure is the barrier height (BH), which is influenced by a variety of parameters like surface preparation techniques, series resistance, interface inhomogeneities, density of interface states/traps or dislocations, impurity concentration of the semiconductor, temperature, applied bias etc. The crystallography and morphology of metallic over-layers on local scale also plays an important role in the band alignment and consequently on their barrier heights. Particularly for liquid metals, interface strain and phase transitions may also contribute to the overall barrier heights. Depending on these parameters, different types of current transport mechanisms may dominate over the other at a certain temperature and voltage regions. Since these parameters are highly sensitive to BH, the properties may change from diode to diode if the fabrication process were not well optimized. These diverse characteristics make our level of understanding of these diodes far from complete and hence a challenging problem [1–3].

The silicon (Si) based Schottky diode plays an important role in integrated circuit technology. Hence, a thorough knowledge of their fundamental characteristics is critical for their rational design. Many experimental and theoretical studies of the current flow mechanism on the metal–Si Schottky barriers have been reported [4–8]. Theoretical models suggest that the band line up in these diodes is due to the combination of intrinsic and extrinsic effects [5]. The influence of these effects needs to be understood for better device fabrications. The technological fabrication process like resistive heating, e-beam, sputtering etc. usually give rise to thermally driven or adsorption driven process, which are extrinsic in nature [9]. The Schottky junction properties are highly sensitive to these processes and thus modify or hinder some basic characteristics of the prepared device. Hence, an alternative is to adopt a different fabrication technology that reduces or eliminates such effects. In this regard, soft contacting methods like liquid metal probes are noteworthy.

The use of mercury (Hg) as a soft metal contact has initiated since long [10]. Recently its popularity has been increased in the study of electron transport property across metal/monolayer/semiconductor junctions [11–13]. The Hg–Si contact is very important for the HgFET and Si on insulator (SOI) material characterization since its barrier is critically influenced by the Hg–Si interface [14]. Its junction formation does not require sophisticated technology and hence the Schottky diode fabrication of this structure is quite easy. Since this fabrication method does not involve vaporization process, there are no non-equilibrium conditions due to heat of condensation, adsorption or metallization between the contact metal and the semiconductor [5]. However, the advantages of such an assembly are numerous [15]. There is no chemical reaction between Hg and Si [16] and so eliminates the chances for an alloy or silicide formation at the

* Corresponding author. Tel.: +91 9470194795.
E-mail address: achammajohn@yahoo.com (A. Bobby).

0921-4526/$ - see front matter © 2013 Elsevier B.V. All rights reserved.
http://dx.doi.org/10.1016/j.physb.2013.08.037

interface. Owing to the simplicity of the assembly, time required for the interface formation is less and minimizes the possible time dependent chemical and electronic changes that may take place on the Si surface.

Investigations on Hg–Si Schottky contacts are mostly dealt with the influence of surface/interface preparation conditions on the Schottky barrier height and interface states at room temperature (RT) [5,17–19]. Up to our knowledge, no reports could be found regarding the *I*–*V* characteristics on such a system over a wide temperature range. Moreover, Hg–Si is a proper system to investigate the phase related behavior of such devices since the melting point of Hg lies in the chosen temperature range of the present investigation.

2. Experimental

The Schottky diodes were fabricated on *n*-type Si ⟨1 0 0⟩ wafers with carrier concentration of the order of 10^{15} cm^{-3} at RT. The crystals were cleaned by wet chemical method, which consists of degreasing steps in boiling trichloroethylene, acetone and isopropanol each followed by a thorough rinse in 18 MΩ-cm de-ionized water. The oxide layers present on the semiconductor surface was stripped off by immersion of the sample in a 1% HF for a few seconds, followed by a thorough rinse in de-ionized water. The cleaned wafer was immediately inserted into the deposition chamber, which was evacuated to a pressure of the order of 10^{-6} Torr prior to metal deposition. Ohmic contacts were made by evaporating 150 nm thick Al metal on the unpolished side of the crystal. On the front polished surface, a fixed teflon capillary arrangement of 2 mm diameter was made, through which pure liquid mercury (Merck, 99.99%) was poured using a medical grade syringe, so that Hg directly comes into touch with the Si surface forming the Schottky contact. The schematic representation of the experimental set up is shown in Fig. 1.

The current–voltage (*I*–*V*) characteristics from 293 K down to 160 K were taken with the help of Keithley 2400 source measurement unit, Lakeshore model 340 temperature controller (±0.1 K) and a close cycle He refrigerator. All the measurements were carried out in a vacuum of the order of 10^{-3} Torr.

3. Results and discussion

The *I*–*V* characteristics of the Hg–*n*Si Schottky diode in the temperature range 160–293 K are shown in Fig. 2. The data shows a clear temperature dependent nature in the whole temperature range with a gap in between 220 and 240 K. The forward current shows a saturating nature at higher voltage regime that is quite often associated with diodes having finite series resistance 'R_s' [20,21]. The reverse bias data shows soft reverse characteristics that are more prominent below 240 K.

For a Schottky barrier diode with an assumption that the current is due to thermionic emission (TE), the relation between the applied

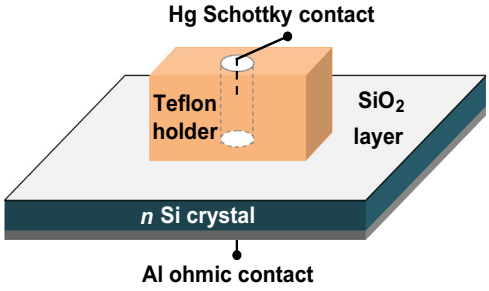

Fig. 1. Experimental schematics of the Hg–*n*Si Schottky diode.

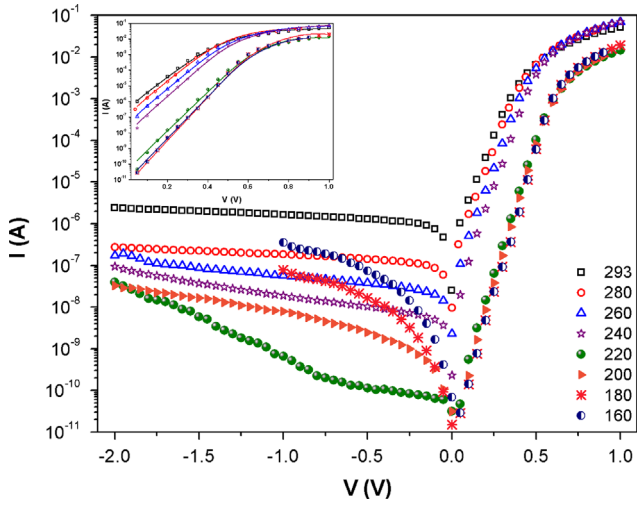

Fig. 2. Experimental *I*–*V* characteristics of Hg–*n*Si Schottky diode at different temperatures. Inset shows forward *I*–*V* characteristics with best fit.

forward bias (*V*) and current (*I*) can be expressed as [22,23]

$$I = I_0\left[\exp\left(\frac{q(V-IR_S)}{nkT}\right)\right]\left[1-\exp\left(\frac{-qV}{kT}\right)\right] \quad (1)$$

where I_0 is the reverse saturation current given by

$$I_0 = AA^*T^2\exp\left(-\frac{q\phi_{b_0}}{kT}\right) \quad (2)$$

Here, R_s is the series resistance, n is the ideality factor, q is the electronic charge, k is the Boltzmann's constant, A is the contact area of the device, A^* is the effective Richardson constant, T is the absolute temperature and ϕ_{b_0} is the zero bias BH. The potential drop IR_s in the neutral region of the semiconductor and back ohmic contact is taken into account by replacing V with V–IR_s in Eq.(1). The ϕ_{b_0} values are determined by the equation below

$$\phi_{b_0} = \frac{kT}{q}\ln\left(\frac{AA^*T^2}{I_0}\right) \quad (3)$$

Here, A^* is the Richardson constant, which is assumed to be equal to 1.12×10^6 A/m^2/K^2 for *n*Si [22] at all temperatures.

Based on Eq. (1), best fit to the forward experimental data was done using PLOT 5.0 software with I_0, n and R_s as input parameters and is shown in the inset of Fig. 2. It shows that the measured data fits quite well with Eq. (1) in the whole temperature regime. The value of reverse leakage current I_{RL} is taken from the reverse *I*–*V* data. The variation of ϕ_{b_0}, n, R_s and I_{RL} parameters with temperature is shown in Figs. 3–5 respectively.

The values of ϕ_{b_0}, n, R_s and I_{RL} (0.5 V) obtained at room temperature are 0.69 eV, 1.79, 9.3 Ω and 1.29×10^{-6} A respectively. According to Schottky model, an abrupt Hg–*n*Si contact at RT should give a BH of 0.45 eV for *n*Si with a band gap, 1.12 eV. However its value changes with thickness of the oxide layer at the interface [16]. The BH value of 0.69 eV in the present case implies a finite amount of oxide layer. The high values of n of 1.79 may be due to the inhomogeneities in thickness and composition of the oxide layer, non-uniformity of the interfacial states etc. at the interface [24]. The ϕ_{b_0} value decreases and n value increases with fall in temperature. A sharp discontinuity is observed for ϕ_{b_0} below 240 K, whereas it is not that prominent in n. This anomalous variation of ϕ_{b_0} and n again points towards the inhomogeneous nature of the interface. The R_s decreases, while I_{RL} first decrease and then increase with a fall in temperature. Here also, similar to ϕ_{b_0}, a sharp discontinuity is observed below 240 K.

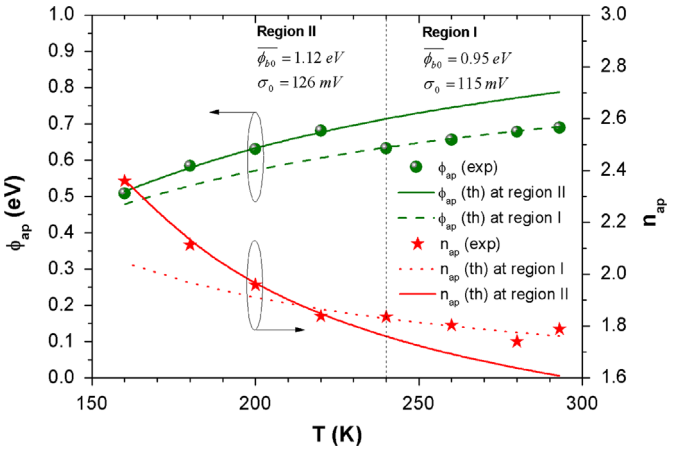

Fig. 3. The temperature dependence of BH and ideality factor. The continuous line represents the data estimated theoretically with $\overline{\phi_{b_0}}$ = 0.95 eV, σ_0 = 115 mV, ρ_2 = 337 mV and ρ_3 = −4.82 mV at region I and $\overline{\phi_{b_0}}$ = 1.12 eV, σ_0 = 126 mV, ρ_2 = 138 mV and ρ_3 = −12.0 mV at region II.

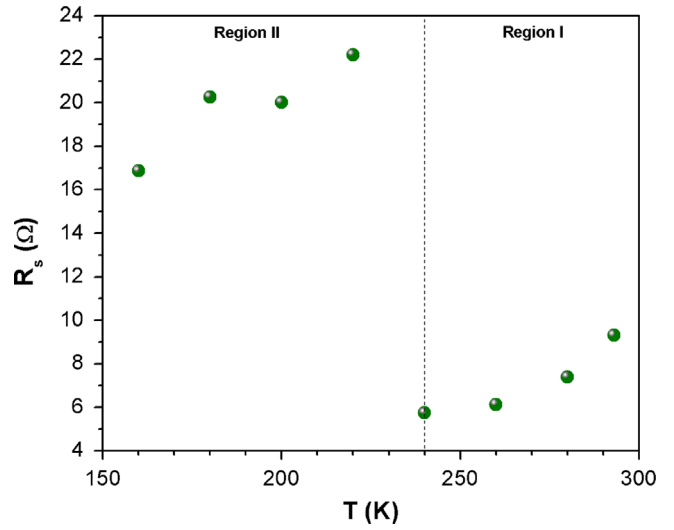

Fig. 4. The variation of series resistance with temperature.

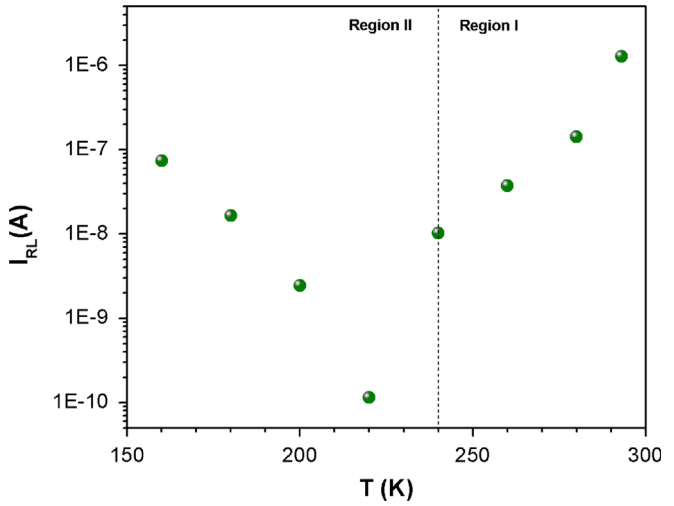

Fig. 5. The variation of reverse leakage current (I_{RL}) with temperature.

Taking into account the temperature variations of ϕ_{b_0} and n in Fig. 3 an inhomogeneous interface with Gaussian distribution of barrier was considered. The resulting Schottky contact will have a mean BH $\overline{\phi_{b_0}}$ with standard deviation σ_0 [25–28]. Then the experimental ϕ_{b_0} and n becomes apparent BH (ϕ_{ap}) and apparent ideality factor (n_{ap}) respectively. At V=0, ϕ_{ap} can be expressed as [29,30]

$$\phi_{ap} = \overline{\phi_{b_0}} - \frac{q\sigma_0^2}{2kT} \tag{4}$$

σ_0 is a measure of the barrier homogeneity. It usually has very small temperature dependence and hence can be neglected. According to this model, the deviation from the classical TE theory can be explained by a continuous spatial fluctuation of low and high barriers at interface. The total current across such diode is obtained by integrating the TE current expression with an individual BH and weighted using the Gaussian distribution function. Hence in this approach, the apparent BH is always lower than the mean value of the barrier distribution.

Similarly, the variation of the ideality factor n_{ap} with temperature is given by [31]

$$\left(\frac{1}{n_{ap}} - 1\right) = -\rho_2 + \frac{q\rho_3}{2kT} \tag{5}$$

Here ρ_2 and ρ_3 are the voltage deformation on the BH distribution, where ρ_2 is the voltage coefficient of the mean BH and ρ_3 is the voltage coefficient of the standard deviation. According to Eqs. (4) and (5), a plot of $(n^{-1}-1)$ against $1/T$ should be a straight line with the slope and y-axis intercept giving ρ_2 and ρ_3 values. The value of ρ_3 indicates that an increase in bias homogenize the BH distribution. The experimental plots of ϕ_{ap} and $(1/n_{ap}-1)$ versus $1/T$ are shown together in Fig. 6. Here, two linear regions with a discontinuity below 240 K could be clearly observed in both the plots that suggest double Gaussian BH distributions in the 160–293 K temperature range. According to this nature, the data is divided into two regions where the 293–240 K range is referred to as region I and 220–160 K range as region II. Taking the linear fit in region I, the values of $\overline{\phi_{b_0}}$ (which is the activation energy E_a) and σ_0 were determined as 0.95 eV and 115 mV respectively from the slope and intercept. Similarly, the values of ρ_2 and ρ_3 were obtained as 337 mV and −4.817 mV respectively from the $(1/n_{ap}-1)$ versus $q/2kT$ plot. In region II, the respective values of $\overline{\phi_{b_0}}$, σ_0, ρ_2 and ρ_3 are 1.115 eV, 126 mV, 138 mV and −12.0 mV.

From the values of $\overline{\phi_{b_0}}$ and σ_0 values, percentage of deviation of ϕ_{ap} from the $\overline{\phi_{b_0}}$ due to inhomogeneity in our device in both the regions was calculated as 12.0%. Now considering Eqs. (2) and (4), the expression for the modified Richardson plot is written as

$$\ln\left(\frac{I_0}{T^2}\right) - \left(\frac{q^2\sigma_0^2}{2k^2T^2}\right) = \ln(AA^{**}) - \left(\frac{q\overline{\phi_{b_0}}}{kT}\right) \tag{6}$$

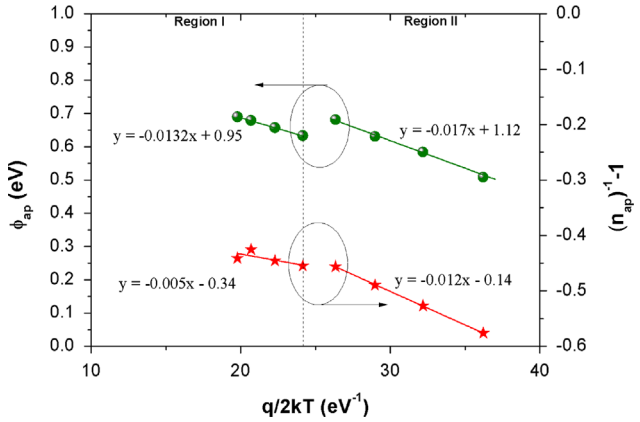

Fig. 6. Zero bias apparent BH and apparent ideality factor versus 1/T curves according to Gaussian distributions in regions I and II with their respective $\overline{\phi_{b_0}}$, σ_0, ρ_2 and $\rho_3$values.

Here, the $\frac{1}{2}(q\sigma_0/kT)^2$ term is the correction factor according to the Gaussian distribution of the BHs with a modified Richardson constant A^{**}. Using the experimental I_0 data, a plot of $\ln[(I_0/T^2) - q^2\sigma_0^2/2k^2T^2]$ versus $1/T$ should give a straight line with slope directly yielding mean BH $\overline{\phi_{b_0}}$ and the intercept at the ordinate $(=\ln AA^{**})$ giving A^{**} for a known diode area A. Two such plots were drawn in Fig. 7 corresponding to two different values of σ_0 in the two regions (115 mV in region I and 129 mV in region II). The slope of the linear fit of this plot gives $\overline{\phi_{b_0}}$ in the respective temperature range. The mean BH values obtained are 0.95 eV in the 293–240 K range and 1.12 eV in the 220–160 K range. These values match exactly with those obtained from the ϕ_{ap} versus $1/T$ plot in Fig. 6. Similarly, A^{**} values obtained are 1.15×10^6 A/m^2/K^2 in the 293–240 K range and 1.33×10^6 A/m^2/K^2 in the 220–160 K range. Both the values are close to the known theoretical value of 1.12×10^6 A/m^2/K^2 of nSi [22].

Using Eqs. (4) and (5), the values of ϕ_{b_0} and n at each temperature was calculated in the two regions with their corresponding $\overline{\phi_{b_0}}$, σ_0, ρ_2 and ρ_3 values and is plotted in Fig. 4, which shows a good fit to the measured data. The standard deviation here, which is a measure of barrier inhomogeneity, is not small compared to the mean BH value in both the regions (~12%). This indicates an inhomogeneous interface with low and high barriers. At low temperatures, number and energy of electrons will be less and hence cannot surmount high barriers. However, under the application of bias, the carriers prefer to flow through the low barrier regions resulting in lower barrier heights with larger ideality factor. At high temperatures, as the bias voltage increases, the smaller barrier height regions get pinched off gradually on account of interaction between barriers. At these temperatures, more and more electrons with sufficient energy will be available to cross this high barrier [31]. This explains the generally observed and well-documented trend often associated with inhomogeneous diodes that the effective barrier height decrease as the ideality factor becomes larger. The soft behavior of the reverse leakage current could also be the result of such inhomogeneous interfaces, where the current in this direction may be dominated by the current that is flowing through the low-BH patches. It shows a decreasing trend in region I where as an increasing trend in region II.

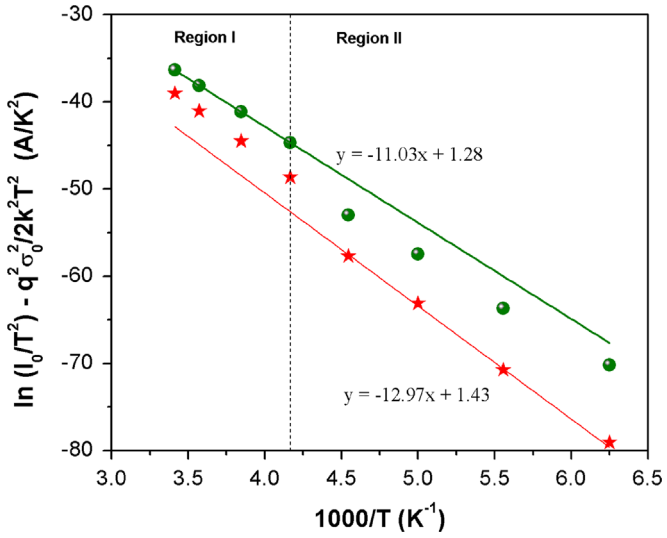

Fig. 7. Modified Richardson (activation energy) plots. The values of $\overline{\phi_{b_0}}$ obtained are 0.95 eV in region I and 1.12 eV in region II.

The double Gaussian distribution of barriers was reported earlier for many metal–Si systems [32–35]. However, contradictory to our results the observed transition temperature was below 200 K. On the other hand, here, the A^{**} values obtained in both the regions are close to each other and is in agreement with the theoretical value of nSi. So the observed variation below 240 K could only be due to the variation in the mean BH ϕ_{b_0}. Considering this along with the melting point of Hg of 234.28 K [36], the origin of the transition below 240 K in the Hg–nSi system could be ascribed as the property of the Hg metal itself, rather than that of the semiconductor, Si.

Hg is a metal with a lot of distinctive physical and chemical properties. Even though it is officially classed as a mineral species for historical reasons, it does not satisfy the normal criteria to be a valid mineral since it occurs as a liquid at room temperature. Its crystalline structure as a solid is rhombohedral [37] and the electrical resistivity is strongly anisotropic. Nevertheless, its structure in the liquid form still remains inconclusive. The Hg freezing point (melting point) of 234.28 K is the lowest of all metals. Interestingly, the transition temperature in our case is also in between 220 and 240 K. Hence the observed double Gaussian nature is attributed to the phase transition of mercury from liquid to solid state. When the metal is in liquid form, the atoms in this phase are loosely bound and could not make a proper link on the topmost semiconductor layer to form a perfect contact (Fig. 8). This give rise to interface states, which can affect Fermi level pinning and consequently the barrier heights to different values depending on the number and kinds of such states. In the solid phase, this interfacial bonding will be more rigid and hence a higher value of barrier height can be expected. The values of mean BH obtained in the present case (0.95 eV for liquid and 1.12 eV for solid) are a clear evidence for the aforementioned explanation. Since a higher value of mean BH indicates a more homogeneous interface, it could be inferred that solid Hg–Si interface to be more homogeneous than liquid Hg–Si interface.

The solidification of any substance is a first order phase transition by the rearrangement of its crystal lattice. It consists of changes in the inter-atomic distance and the angles between lattice planes. When Hg solidifies, it crystallizes in a form that is different from its liquid state. As a result, there would be a change in the lattice constants and the symmetry of the crystal grains. Evidently the planes of the crystal grains will have different indices and orientations at the interface before and after its

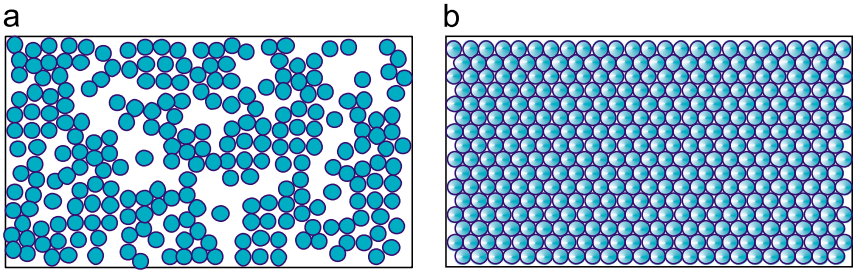

Fig. 8. Microscopic view of the element mercury: (a) in the liquid state and (b) in solid form (below 234.28 K).

melting point. These restructuring and re-ordering at the interface might possibly be perturbing the interfacial bonding and band structure of mercury on solidification. This changes the existing barrier height distribution and causes double Gaussian BH distribution. The restructuring and re-ordering is also associated with change in temperature and modifies accordingly the interface state density. This gets reflected in the series resistance also [38], where a decreasing effect is observed with decrease in temperature below 240 K.

4. Conclusion

Investigation of Hg contacts on n type silicon with $\langle 1\,0\,0\rangle$ orientation was carried out in the temperature range of 160–300 K by analyzing the temperature dependent I–V characteristics according to thermionic emission model with Gaussian distribution of barrier heights. The room temperature barrier height is found to be 0.69 eV having an ideality factor of 1.79. The large value of ideality factor could be due to the presence of native oxide layers with in homogeneous interfaces. Below 240 K, discontinuities were observed in barrier height, ideality factor and series resistance. The ϕ_{ap} and $(n^{-1}-1)$ versus $1/T$ plot give two different slopes, one in the 293–240 K range (region I) and the other in 220–160 K range (region II). However, the value of modified Richardson constant obtained in both the regions is close and is in agreement with the theoretical value of nSi. Hence it was concluded that the discontinuities that prevails below 240 K and the existence of double Gaussian BH distribution are the outcome of the band realignment at the interface due to the phase transition of mercury from its liquid state to solid.

Acknowledgment

Authors are grateful for the fruitful discussions with Dr. D. Kanjilal and Dr. D. Kabiraj. The technical support from Mr. Abhilash S.R (IUAC, India) is also acknowledged. AB would like to thank Department of Science and Technology, India for the financial support under Grant no: SR/WOS-A/PS-26/2009.

References

[1] L.J. Brillson, Y. Lu, J. Appl. Phys. 109 (2011) 121301.
[2] D. Bauza, G. Pananakakis, J. Appl. Phys. 69 (1991) 3357.
[3] E.H. Rhoderick, R.H. Williams, Metal–Semiconductor Contacts, 2nd ed., Clarendon Press, Oxford, 1988.
[4] J.H. Evans-Freeman, M.M. El-Nahass, A.A.M. Farag, A. Elhaji, Microelectron. Eng. 88 (2011) 3353.
[5] M. Wittmer, J.L. Freeouf, Phys. Rev. Lett. 69 (1994) 2701.M. Wittmer, J.L. Freeouf, Europhys. Lett. 26 (1994) 135.
[6] J. Tersoff, Phys. Rev. Lett. 52 (1984) 465.
[7] D.R. Heslinga, H.H. Weitering, D.P. van der Werf, T.M. Klapwijk, T. Hibma, Phys. Rev. Lett. 64 (1990) 1589.
[8] R.T. Tung, A.F.J. Levi, J.P. Sullivan, F. Schrey, Phys. Rev. Lett. 66 (1991) 72.
[9] E. Ohta, K. Kakishita, H.Y. Lee, T. Sato, M. Sakata, J. Appl. Phys. 65 (1989) 3928.
[10] J.A. Medley, Br. J. Appl. Phys. 4 S (1953) 28.
[11] O. Yaffe, L. Scheres, L. Segev, A. Biller, I. Ron, E. Salomon, M. Giesbers, A. Kahn, L. Kronik, H. Zuilhof, A. Vilan, D. Cahen, J. Phys. Chem. C 114 (2010) 10270.
[12] A. Salomon, T. Boecking, C.K. Chan, F. Amy, O. Girshevitz, D. Cahen, A. Kahn, Phys. Rev. Lett. 95 (2005) 266807.
[13] H.J. Hovel, Solid-State Electron. 47 (2003) 1311.
[14] J.Y. Choi, D.K. Schroder, IEEE Trans. Electron. Devices 15 (2006) 769.
[15] A.J. Mathai, IEEE Trans. Electron. Devices 58 (2011) 4283.
[16] J.Y. Choi, S. Ahmed, T. Dimitrova, J.T.C. Chen, IEEE Trans. Electron. Devices 51 (2004) 1380.
[17] P.J. Severin, G.J. Poodt, J. Electrochem. Soc. 119 (1972) 1384.
[18] Q. Wang, D. Liu, J.T. Virgo, J. Yeh, R.J. Hillard, J. Vac. Sci. Technol. A,Vac. Surf. Films 18 (2000) 1308.
[19] A.J. Mathai, K.D. Patel, R. Srivastava, Thin Solid Films 518 (2010) 2695.
[20] S. Chand, S. Bala, Appl. Sur. Sci. 252 (2005) 358.
[21] S. Chand, J. Kumar, J. Appl. Phys. 82 (1997) 5005.
[22] S.M. Sze, K.K. Ng, Physics of Semiconductor Devices, 3rd ed., Wiley Interscience (2007) 793.
[23] D. Donoval, A. Chvala, R. Sramaty, J. Kovac, E. Morvan, Ch. Dua, M.A. DiForte-Poisson, P. Kordos, J. Appl. Phys. 109 (2011) 063711.
[24] M. Okutan, F. Yakuphanoglu, Microelectron. Eng. 85 (2008) 646.
[25] R.T. Tung, Phys. Rev. B 45 (1992) 13509.
[26] A. Kumar, K. Asokan, V. Kumar, R. Singh, J. Appl. Phys. 112 (2012) 024507.
[27] J.H. Werner, H.H. Güttler, J. Appl. Phys. 69 (1991) 1522.
[28] A.J. Mathai, K.D. Patel, R. Srivastava, Thin Solid Films 518 (2010) 4417.
[29] S. Chand, J. Kumar, J. Appl. Phys 82 (5005) (1997);
S. Chand, S. Bala, Appl. Surf. Sci. 252 (2005) 358;
S. Chand, J. Kumar, Appl. Phys. A: Mater. Sci. Process 65 (1997) 497.
[30] J. Osvald, J. Appl. Phys. 85 (1935) (1999);
E. Dobrocka, J. Osvald, Appl. Phys. Lett. 65 (1994) 575;
J. Osvald, Solid-State Electron. 50 (2006) 228.
[31] N. Yıldırım, K. Ejderha, A. Turut, J. Appl. Phys. 108 (2010) 114506.
[32] S. Chand, J. Kumar, Semicond. Sci. Technol. 11 (1996) 1203.
[33] İ. Taşçıoğlu, U. Aydemir, Ş. Altındal, J. Appl. Phys. 108 (2010) 064506.
[34] O. Pakma, N. Serin, T. Serin, Ş. Altındal, J. Appl. Phys. 104 (2008) 014501.
[35] Y.L. Jiang, G.P. Ru, Lu Fang, X.P. Qu, Li Bing-Zong, Yang Simon, J. Appl. Phys. 93 (2003) 866.
[36] CRC Handbook of Chemistry and Physics, 93rd Ed. (2012–2013).
[37] C.S. Barrett, Acta Crystallogr. 10 (1957) 58.
[38] D.E. Yildiz, S. Altindal, Microelectron. Eng. 85 (2008) 289.